Diurnal and nocturnal distribution of stratospheric NO: from solar and stellar occultation measurements in the Arctic vortex' Comparison with models and ILAS satellite measurements

Sébastien Payan, Claude Camy-Peyret, P. Jeseck, T. Hawat, Michel Pirre, Jean-Baptiste Renard, Claude Robert, Franck Lefèvre, H. Kanzawa, Y. Sasano

Diurnal and nocturnal distribution of stratospheric NO₂ from solar and stellar occultation measurements in the Arctic vortex: Comparison with models and ILAS satellite measurements

S. Payan,[1] C. Camy-Peyret,[1] P. Jeseck,[1] T. Hawat,[1,2] M. Pirre,[3,4] J.-B. Renard,[3] C. Robert,[3] F. Lefèvre,[5,6] H. Kanzawa,[7] and Y. Sasano[7]

Abstract. NO₂ mixing ratio profiles were measured at sunset between 14 and 30 km using the Limb Profile Monitor of the Atmosphere (LPMA) experiment and during the night between 13 and 31 km using the Absorption par Minoritaires Ozone et NOₓ (AMON) experiment inside the Arctic vortex, both on February 26, 1997. Coinciding profiles measured by the Improved Limb Atmospheric Spectrometer (ILAS) instrument on board ADEOS have been used to check the consistency between the satellite and balloon profiles for NO₂, O₃, and HNO₃. A box model has been used for the photochemical correction of the LPMA NO₂ profiles at sunset. The resulting NO₂ balloon-borne profiles of LPMA and AMON are compared to each other after accounting for the day/night photochemical variation using the box model initialized with measurements. The comparisons thus performed show an average difference less than 9% between the two measurements (considered to sample similar air masses) when the box model is initialized with little chlorine activation (i.e., when the major burden of chlorine is stored in ClONO₂) for a 1 day integration. The comparison with the Reprobus 3-D chemistry transport model (CTM) seasonal simulations clearly confirms an underestimation of NO₂ by the model below 25 km, in the altitude range where aerosols lead to a complete removal of NOₓ in the model. Recent updates of rate coefficients for conversion of HNO₃ into NO₂ only slightly improve the NO₂ model results in vortex conditions. These results suggest that a source of NO₂ is still lacking in the CTM.

1. Introduction

NO₂ plays an important role in the lower stratosphere because it is involved both in chemical processes leading to ozone destruction and in processes buffering chlorine activation through the formation of the mixed reservoir ClONO₂ [*Brasseur and Solomon*, 1986]. Previous measurements at midlatitudes, for air unaffected by polar stratospheric clouds but under different aerosol loading conditions [*Sen et al.*, 1998; *Kondo et al.*, 1997; *Webster et al.*, 1994] have suggested an incomplete understanding of the factors regulating the NO₂ concentration below 30 km. In winter conditions, measurements of NO₂ inside the Arctic polar vortex [*Lary et al.*, 1997; *Wetzel et al.*, 1997] show a disagreement with three-dimensional (3-D) chemistry transport model simulations in the lower stratosphere below 22 km altitude. Measurements of NO₂ profiles in the polar vortex are not easily performed, however, and the available database [*Glatthor et al.*, 1998; *Newchurch et al.*, 1996] does not provide an adequate sampling of the photochemical cycle.

In order to complement previous observations and to document the observed disagreement, we present new measurements of the NO₂ vertical profiles inside the polar Arctic vortex at the same location but for different times of the diurnal/nocturnal cycle. Indeed, for the first time, NO₂ profile measurements have been performed during the day (late afternoon and sunset) and 5 hours later during the night using respectively the balloon-borne instruments Limb Profile Monitor of the Atmosphere (LPMA) and Absorption par Minoritaires Ozone et NOₓ (AMON), in the framework of the Improved Limb Atmospheric Spectrometer (ILAS) validation balloon campaign in February 1997 [*Kanzawa et al.*, 1997] from Kiruna, Sweden (68°N, 21°E). AMON measurements of O₃; LPMA measurements of O₃, HCl, and HNO₃; and ILAS [*Sasano et al.*, 1999] measurements of NO₂, O₃ and HNO₃ obtained for February 26, 1997, are also presented.

[1]Laboratoire de Physique Moléculaire et Applications, Université P. et M. Curie, Paris, France.

[2]Now at University of Balamand, Faculty of Engineering, Beirut, Lebanon
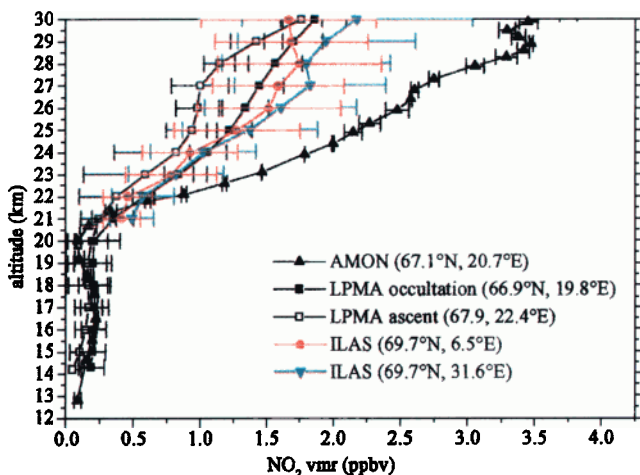
[3]Laboratoire de Physique et de Chimie de l'Environnement, CNRS, Orléans, France.

[4]Also at Université d'Orléans, Orléans, France.

[5]Centre National de Recherche Météorologique, Météo-France/CNRS, Toulouse, France.

[6]Now at Service d'Aéronomie du CNRS, Université P. et M. Curie, Paris, France.

[7]National Institute for Environmental Studies, Tsukuba, Japan.

Plate 1. NO₂ vertical profiles on February 26, 1997, retrieved from ILAS satellite measurements (red circles and blue inverted triangles), LPMA ascent measurements (white boxes), LPMA occultation measurements (black boxes), and AMON nighttime measurements (black triangles). The LPMA measurements are photochemically corrected (SZA = 83° for ascent, SZA = 90° for occultation).

NO₂, O₃, HCl, and HNO₃ measurements are compared with the output of the Reprobus 3-D chemistry transport model (CTM) [*Lefèvre et al.*, 1998] and with the output of a box model constrained with measurements of AMON and LPMA. The box model output has also been used for intercomparison of the LPMA and AMON NO₂ profiles and for the photochemical correction of the LPMA profiles. The results are discussed in terms of nitrogen and chlorine partitioning. The effect of recent updates of rate coefficients for gas-phase conversion of HNO₃ into NO₂ has been considered.

2. Observation Methods and Vertical Profiles

As a remarkable achievement of the Centre National d'Etudes Spatiales (CNES) launching team, the two flights reported here took place in the late afternoon and the early night of February 26, 1997, from the Swedish launching base of the European
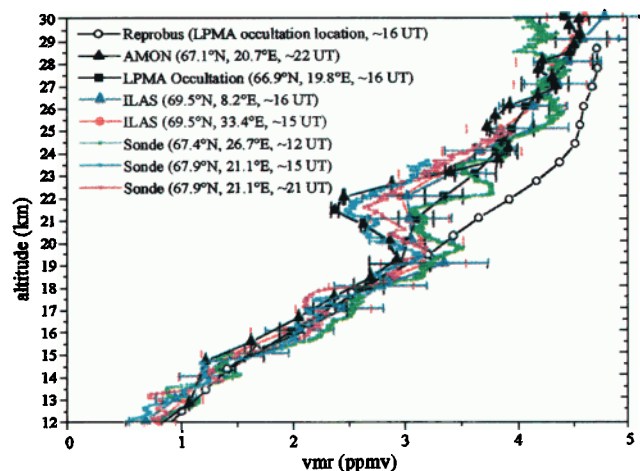
Plate 2. Vertical profiles of O₃ measured by LPMA (black boxes), AMON (black triangles), soundings (green, magenta, and cyan boxes), and ILAS (blue triangles and red circles) compared to Reprobus CTM modeling.
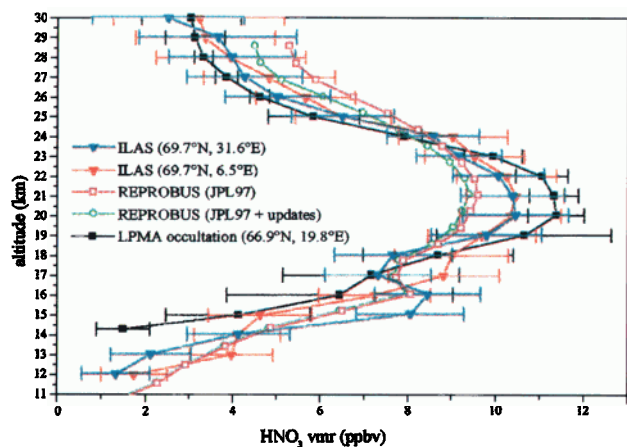
Plate 3. LPMA HNO₃ occultation measurements, corresponding Reprobus modeling with JPL97 and with updated rate constants, and ILAS measurements for February 26, 1997.

Space Research Range (ESRANGE) (~68°N, ~21°E). The LPMA experiment has collected infrared spectra in the late afternoon for increasing solar zenith angles (SZA) from 13 30 UT to 14 59 UT during ascent (SZA < 90°) and from 15 00 UT to 15 40 UT during occultation (SZA > 90°). The AMON experiment collected UV-visible spectra during the night from 21 05 UT to 22 11 UT. Two measurements were performed by ILAS rather close to Kiruna (around 500 km) on the same day at 14 26 and 16 07 UT. The LPMA and AMON NO₂ vertical profiles retrieved during the two flights of February 26 for the corresponding time periods are presented in Plate 1 together with the coincident ILAS measurements. The different measurements are described below.

2.1. LPMA Observations

The LPMA is a remote sensing infrared Fourier transform instrument operating in absorption against the Sun [*Camy-Peyret*, 1995]. With its high spectral resolution and sensitivity, the retrieval of vertical profiles of trace species having stratospheric mixing ratios as small as 0.1 ppbv is possible. During the flight, the Sun was encountered above a rather elevated cloud deck at about 10 km. The first complete interferograms (after proper setting of the gains of the preamps for each channel) were obtained just above 13 km. From that point on, the primary pointing system, the heliostat, the interferometer, and all the ancillary equipment performed nominally during ascent, float, and occultation up to loss of Sun, again behind the high cloud cover (~13 km). The 170 recorded spectra show sufficient absorption by NO₂ for precise retrieval in the appropriate micro-window around 2914.6 cm⁻¹. The LPMA flight observations started at 13 30 UT (the balloon was at an altitude of 14.2 km during its ascent), the float was reached at 15 00 UT and occultation measurements (SZA > 90°) were recorded until loss of Sun at 15 40 UT. Around 120 spectra were recorded during ascent (SZA < 90°), and around 50 during occultation. Tables 1a and 1b give the altitude, location, and time (UT) for a few representative spectra recorded during ascent and during occultation, respectively.

A global fit algorithm [*Carlotti*, 1988] associated with an efficient minimization algorithm of the Levenberg-Marquardt type [*Press et al.*, 1992] is used for the retrieval. This retrieval algorithm [*Payan et al.*, 1998] allows us to retrieve vertical profiles from both ascent and occultation data. The retrieval from

Table 1a. Latitude (Degrees North), Longitude (Degrees East), Solar Zenith Angle (SZA), Time, and Local Time of LPMA Ascent Measurements for Selected Balloon Atitudes z

Latitude	Longitude	SZA, deg	Time, UT	Local Time hours	Z, km
67.90	21.66	81.76	13 30	15 00	14.20
67.94	22.23	82.94	13 45	15 15	18.98
67.97	22.92	84.01	13 57	15 27	22.98
67.98	23 77	85.17	14 10	15 40	26.60
67.97	24.63	86.39	14 23	15 53	29.50
67.90	26 77	89.76	14 56	16 26	31.86

ascent data is only possible when using a global fit method because the spectral information is strongly integrated along the vertical in the ascent spectra. In all cases the molecular parameters used in the forward model are extracted from the HITRAN96 database. Because of the different viewing geometries for ascent and occultation spectra and because of the inhomogeneities in the geophysical fields inside and around the Arctic vortex, we have decided to perform separate retrievals for the two geometries. The volume mixing ratio profiles (together with the corresponding error) have been retrieved from the selected lowest observation points (14.2 km for ascent and 14.3 km for occultation, with volume mixing ratio (vmr) values at these levels extrapolated from values at the two higher retrieval altitudes) up to the highest balloon altitude (float at 30 km) with a vertical sampling of 1 km.

The rapid time variation in the concentration of NO$_2$ at sunset, if not properly accounted for, will produce errors in the retrieval of this species from solar occultation measurements [Kerr et al., 1987; Russel et al., 1988; Newchurch et al., 1996]. The variation of NO$_2$ is mainly governed by the reaction of NO with O$_3$, the reaction of NO$_2$ with ClO, and by the photolysis of NO$_2$. Hence accurate knowledge of the local values of O$_3$, temperature, and radiation field is required to calculate the variation of NO$_2$ along the occultation line of sight. The vertical profile of O$_3$ has been measured by the AMON and the LPMA experiments. These measurements are presented in Plate 2 together with three soundings performed the same day. The measurements are in good agreement below 19 km and above 23 km (differences less than 10%), whereas some differences are observed between 19 and 23 km. The AMON profile and the soundings performed from Kiruna show more structure than the LPMA profile or the sounding performed from Sodankyla (Finland). Taking into account the locations and the times of each measurement, these differences in a rather narrow altitude range are probably due to small-scale geophysical variability (proximity of the vortex edge, leewaves, transport).

We have used the LPCE time-dependent photochemical box model [Ramaroson et al., 1992; Renard et al., 1996] to calculate the diurnal variation of NO$_2$. The model has been constrained with the AMON measurements of NO$_2$, and the LPMA measurements of O$_3$, HCl, H$_2$O, N$_2$O, CH$_4$, and HNO$_3$. Although simultaneous observations of HCl and ClONO$_2$ have been performed previously with the LPMA instrument [Payan et al., 1998], the loss (during ground testing) of a KCl beamsplitter (replaced by a CaF$_2$ one) unfortunately prevented us from covering the 780 cm^{-1} feature of ClONO$_2$ which was not available for constraining the box model. The accuracy with which the model calculates the relative variation of NO$_2$ is a critical element for correcting solar-occultation retrievals. We have used the box model to describe the altitude dependent

diurnal variation of NO$_2$ relative to two reference values, SZA=83° for ascent (corresponding to 20 km altitude) and SZA=90° for occultation measurements. Box model derived correcting factors have been used in the LPMA global fit retrieval algorithm to correct the NO$_2$ vmr at each layer boundaries for each line of sight during ascent and on each side of the tangent point along the line of sight for occultation. The vmr differences are less than 6% at any level as compared to a photochemically noncorrected profile. The resulting NO$_2$ vertical profiles (ascent and occultation) are thus corresponding to the chosen reference solar zenith angles (of 83° for ascent and 90° for occultation) for each altitude.

2.2. AMON Observations

AMON is composed of a 20-cm Cassegrain telescope with a 1-m focal length, a grating spectrometer designed for continuous coverage of the UV and visible wavelength domains, and a CCD detector 385 by 578 pixels [Robert, 1992; Naudet et al., 1994]. Spectra are sampled in five bands at 0.14 nm per pixel in four visible bands and 0.18 nm per pixel in one UV band. During stratospheric flight, the instrument was mounted on board the stabilized platform of Geneva Observatory. Observations were made using the stellar occultation method, which allows retrieval of slant column densities of atmospheric species for different lines of sight below the balloon horizon. An onion-peeling inversion technique is used to derive the vertical distribution of the trace species and the aerosol extinction coefficient.

NO$_2$ absorption was observed by AMON between 400 and 475 nm, where its spectral signature is easily recognized. The slant columns were retrieved by applying a differential method, which allows the Rayleigh, aerosols, and ozone contributions to be removed by high-pass filtering, and by using the NO$_2$ cross sections measured by Harder et al. [1997]. The use of new NO$_2$ low-temperature cross sections (J.P. Burrows et al., private communication, 1998; Web site http://www.iup.physik.uni-bremen.de/gruppen/molspec.html) will not change the retrieved profile by more than 2%. The ozone contribution was derived from the Chappuis band between 550 and 625 nm using the O$_3$ cross sections of J. Brion (Reims University, private communication, 1997). A detailed description of the data processing is given by Renard et al. [1996].

The AMON flight observations started at 21 05 UT and ended at 22 11 UT, when the balloon was at float altitude (around 31.4 km). The star used for the occultation was Rigel. Around 100 spectra were recorded. Table 1c gives the altitude, location, and time (UT) for a few representative spectra recorded by AMON.

Table 1b. Latitude (Degrees North), Longitude (Degrees East), Solar Zenith Angle (SZA), Time, and Local Time of LPMA Occultation Measurements for Selected Tangent Atitudes H$_t$

Latitude	Longitude	SZA, deg	Time, UT	Local Time hours	H$_t$, km
67.85	26.77	90.10	14:59	15:29	31.94
67.29	23.89	91.68	15:13	16:43	29.16
67.20	23.21	92.03	15:16	16:46	27.83
67.01	21.51	92.94	15:24	16:54	23.60
66.93	20.47	93.48	15:28	16:58	20 37
66.89	19.44	94.03	15:33	17:03	16 81
66.87	18.78	94.39	15:36	17:06	14.31

Table 1c. Latitude (Degrees North), Longitude (Degrees East), Time, and Local Time of the nighttime AMON Measurements for Selected Tangent Atitudes H$_t$

Latitude	Longitude	Time, UT	Local Time, hours	H$_t$, km
67.73	27.29	21·28	22·58	31.38
67 45	25.48	21:38	23:08	29.63
67 24	23.74	21:46	23:16	26.50
67.14	22 32	21:53	23:23	23.10
67.06	20.71	22:00	23:30	18.41
67.01	19.82	22.03	23:33	15.56
67.00	18 49	22.06	23 36	11.31

2.3. Geophysical Conditions

According to the temperature profile encountered during the flight (minimum of 195 K around 21 km), polar stratospheric clouds (PSCs) were not thermodynamically possible (around 3 K above the Nitric Acid Trihydrate (NAT) threshold temperature). Backward trajectory calculations based on analysis data from the European Centre for Medium-Range Weather Forecasts (ECMWF) indicate that PSC formation was possible 9 days before the flight in air masses passing over Kiruna for the 400 K potential temperature level (around 16 km) and 8 days before the flight for the 550 K level (around 22 km). The low concentrations observed between 19 and 22 km in the measured HCl profile (Figure 1) indeed indicate that chlorine activation may have occurred in this altitude range along the trajectories sampled by LPMA, producing a dip in the HCl profile as a result of the depletion of this species through heterogeneous processes. The fact that the low HCl values are not associated with low HF values measured by LPMA during the same flight is an indication that the feature in the HCl profile is not related to outside vortex intrusion but is potentially related either to mesoscale or to leewave PSCs. Analysis of Total Ozone Mapping Spectrometer (TOMS) and TIROS Operational Vertical Sounder (TOVS) ozone column amounts and analysis of the ECMWF potential vorticity (PV) maps (at 12 00, 18 00 and 0 00 UT) indicate that the measurements have been performed in the inner edge of the polar vortex. The LPMA measurements for ascent (reference SZA of 83°) have been performed more inside the vortex than those for occultation (reference SZA of 90°). A significant part of the differences can be assigned to the NO₂ photochemical variation between these two SZA values. But as can be seen from the positions of the tangent points (see Tables 1b and 1c), the air masses sampled by LPMA during occultation are very close to those sampled 5 hours later by AMON, and within this short time period, the variation in the PV field was only minor. So for NO₂, we limit ourselves to the comparison of the occultation LPMA profile which can be directly compared to the AMON profile, provided the photochemical variation between SZA = 90° and the nighttime AMON measurements is properly accounted for by the box model.

2.4. Comparison With ILAS

Global measurements from space are necessary to better understand the disagreement between modeling and measurements. The ILAS is a solar occultation satellite sensor developed by the Environment Agency of Japan to monitor and study the stratospheric ozone layer environment by using an infrared grating spectrometer and a visible grating spectrometer [*Sasano et al.*, 1999]. It was launched on board the Advanced Earth Observing Satellite (ADEOS) in August 1996. Continuous measurements in two high northern or southern latitude bands were performed between November 1996 and June 1997. With its infrared spectrometer, ILAS can measure vertical profiles of O₃, HNO₃, NO₂, N₂O, CH₄, and H₂O. Profiles of aerosol extinction coefficients at four infrared wavelengths are also derived. With its visible spectrometer, covering the molecular oxygen absorption A-band, temperature and pressure profiles are obtained, as well as the aerosol extinction profile at 780 nm. Data processing is based on a nonlinear least squares method for spectral fitting and the onion-peeling method for vertical profiling.

The altitude range for data analysis is from cloud-top to about 60 km, depending on retrieved parameters. The lowest altitude was sometimes limited by insufficient Sun-tracking capability due to very low signal intensity. The measurement region of ILAS was over high-latitude regions (57-73°N and 64-88°S), which changed according to the season. Because of these unique measurement opportunities, ILAS can generate daily height-longitude cross-sectional maps of atmospheric parameters.

The LPMA and AMON measurements presented in this paper took place in the framework of the ADEOS/ILAS validation balloon campaign carried out from Kiruna (Sweden) in February-March 1997. Two measurements were performed by ILAS rather close to Kiruna (around 500 km) on February 26, 1997. This instrument uses the solar occultation technique at sunset, so the NO₂ ILAS measurements can be directly compared to the LPMA measurements corrected for SZA = 90°. A comparison of our measurements of NO₂ with those of ILAS (algorithm version 3.10) bracketing the LPMA ones is given in Plate 1. The ILAS NO₂ vertical profile is given above 21 km. Below that level, the strong correlation between NO₂ and aerosol absorption features lead to an overestimation of NO₂ values due to improper aerosol absorption modeling in the retrieval. It can be seen that the ILAS error bars generated by the current version of the operational algorithm and discussed by *Yokota et al.* [1998] are rather large and do not fully warrant a statistically significant comparison with the AMON and LPMA vertical distributions of NO₂. If we just consider the retrieved ILAS vmr, a good general agreement (average differences less than 12% and 11% for the two ILAS measurements) is found.

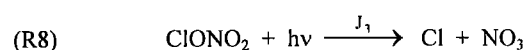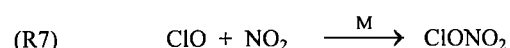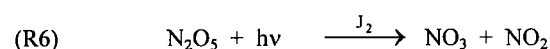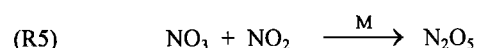In the case of HNO₃ (Plate 3), ILAS measurements are in good agreement with LPMA. The average differences are less
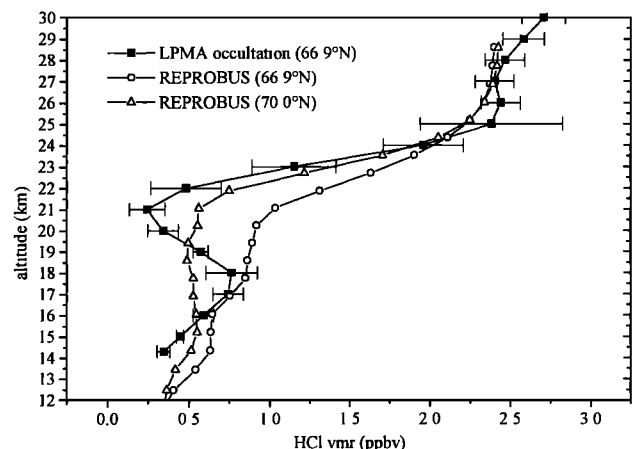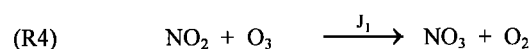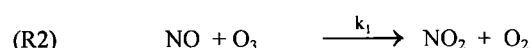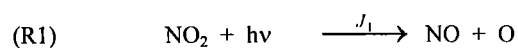

Figure 1. LPMA HCl profile from occultation measurements compared to Reprobus modeling (February 26, 1997). All longitudes pertain to 19.8°E.

than 12% and 15% between the LPMA and the two ILAS measurements, respectively. The differences are larger below 17 km. However, the distance between the measurements (around 500 km) could explain part of these differences. The ILAS ozone measurements (Plate 2) are overall in good agreement with LPMA measurements and an ozone sounding performed the same day from Sodankyla (differences less than 10%). The agreement with AMON measurements and the two Kiruna soundings is about the same, but there is some indication of variability in the altitude range 19-23 km between the two groups of ozone profiles (this may be assigned to small-scale geophysical variability).

3. Study of the NO$_2$ Diurnal Variations Using a Box Model

We have used a photochemical box model to study and reproduce realistically the diurnal and nocturnal variation of NO$_2$ as observed by the LPMA and AMON measurements. A 1 day integration has been performed, from February 26 at 0 00 UT to February 26 at 23 30 UT, assuming that no new chlorine activation occurred during this period. The simulations have been performed for the location of the AMON observations, from 14 to 30 km, in 14 boxes separated by 2 km (between 14 and 20 km altitude) and by 1 km (between 20 and 30 km). We have assumed that for each altitude the two balloon measurements have been performed in the same air mass (this was confirmed by backward trajectories, PV map, and O$_3$ total column map analyses). This hypothesis is reasonable, taking into account the small distance between the measurement locations especially between the occultation LPMA measurements and the AMON measurements as well as the short time difference (less than 6 hours). The model includes a full chemical system, taking into account species of the O$_x$, HO$_x$, NO$_y$, ClO$_y$, and BrO$_y$ families and the long-lived species N$_2$O, CH$_4$, H$_2$O, and CO. Rate constants and dissociation cross sections (taking into account their temperature dependence) are those extracted from *De More et al* [1997]. The total concentrations of the NO$_y$, ClO$_y$, and BrO$_y$ families are fixed, as well as the concentrations of the long-lived species.

The NO$_2$ vmr variation (between the LPMA measurements before or at sunset and the AMON measurements during the night) is mainly governed by the following chemical reactions :

(R1)   NO$_2$ + hv $\xrightarrow{J_1}$ NO + O

(R2)   NO + O$_3$ $\xrightarrow{k_1}$ NO$_2$ + O$_2$

(R3)   NO + ClO $\xrightarrow{k_2}$ NO$_2$ + Cl

(R4)   NO$_2$ + O$_3$ $\xrightarrow{J_1}$ NO$_3$ + O$_2$

(R5)   NO$_3$ + NO$_2$ $\xrightarrow{M}$ N$_2$O$_5$

(R6)   N$_2$O$_5$ + hv $\xrightarrow{J_2}$ NO$_3$ + NO$_2$

(R7)   ClO + NO$_2$ $\xrightarrow{M}$ ClONO$_2$

(R8)   ClONO$_2$ + hv $\xrightarrow{J_1}$ Cl + NO$_3$

The first three reactions lead to a fast equilibrium between NO and NO$_2$ during the day:

$$\frac{[NO]}{[NO_2]} = \frac{J_1}{k_2[ClO] + k_1[O_3]}$$

During sunset, NO is quickly converted to NO$_2$. Let us define

[NO$_x$] = [NO] + [NO$_2$]

In the conditions studied in the paper (high SZA, Arctic vortex), the evolution of this sum during the late afternoon is mainly governed by the last two equations (R7) and (R8), which lead to the decrease of [NO$_x$] until sunset, while N$_2$O$_5$ photolysis (R6) has a negligible effect on the [NO$_x$] variation during the day because of the vortex conditions. During the night, reactions (R4) and (R5) become dominant in the variation of this sum for low ClO concentrations. In the case of high ClO concentrations, the ClO + NO$_2$ reaction is dominant and leads to very small values of NO$_2$. Let us define [NO$_x$ (90°)] as the NO$_x$ concentration for SZA = 90°. Like *Flaud et al.* [1998], we can show that the [NO$_x$] time variation during the night satisfies the following relation :

$$[NO_x] = [NO_x (90°)] \exp(-2k_3[O_3]\Delta t)$$

The evolution of NO$_2$ between the times of the measurements is therefore strongly dependent on the O$_3$ concentration, the temperature, and the degree of chlorine activation. The O$_3$ vmr has been measured by LPMA and AMON, the temperature is known from actual meteorological soundings the day of the flight, and the LPMA HCl measurements allow us to initialize the ClO$_y$ species defined as [ClO$_y$] = [ClO] + 2[Cl$_2$O$_2$] + [ClONO$_2$] + [HOCl] + [OClO]. We can consider that, with a good approximation, this value is equal to [ΣCl] - [HCl] - [Cl$_{org}$], where [ΣCl] is the total stratospheric chlorine burden and [Cl$_{org}$] is the total organic chlorine (source species). These latter values have been taken from the Reprobus CTM (discussed in the next section) for the corresponding day of the measurements. The partitioning has been chosen so that the box model reproduces reasonably well the LPMA and AMON measurements.

The box model was first initialized with the chlorine partitioning given by Reprobus. But below 25 km the box model NO$_2$ vmr was smaller than the measurements and was very similar to Reprobus results. Several sets of chlorine partitioning were then tested, HCl being initialized with LPMA measurements. The best agreement is obtained when values of ClO and Cl$_2$O$_2$ are initialized to zero (at midnight) and when only very small values of HOCl and OClO are retained. This is consistent with the low mixing ratio of OClO (~35 pptv at 23 km) derived from the AMON spectra. Thus, only the case with low chlorine activation allows us to reproduce the measurements with the box model. Under these conditions, inorganic chlorine is mainly partitioned between ClONO$_2$ and HCl.

No aerosols have been considered in the box model, since for all our simulations, an aerosol load similar to what was measured in the Arctic vortex in 1997 leads only to small NO$_2$ variations over the period of our measurements (1 hour between ascent and occultation of LPMA, 5 hours between LPMA and AMON). Aerosols, however, do play a role for longer integration times in the absolute level of NO$_2$, HNO$_3$, and ClONO$_2$ due to denoxification, denitrification, and heterogeneous conversion of N$_2$O$_5$ and ClONO$_2$.

In Figure 2, we present the LPMA and AMON results for four altitudes together with the box model simulation producing the best fit with observations. As can be seen, the agreement of the box model calculations (assuming no aerosols) and the
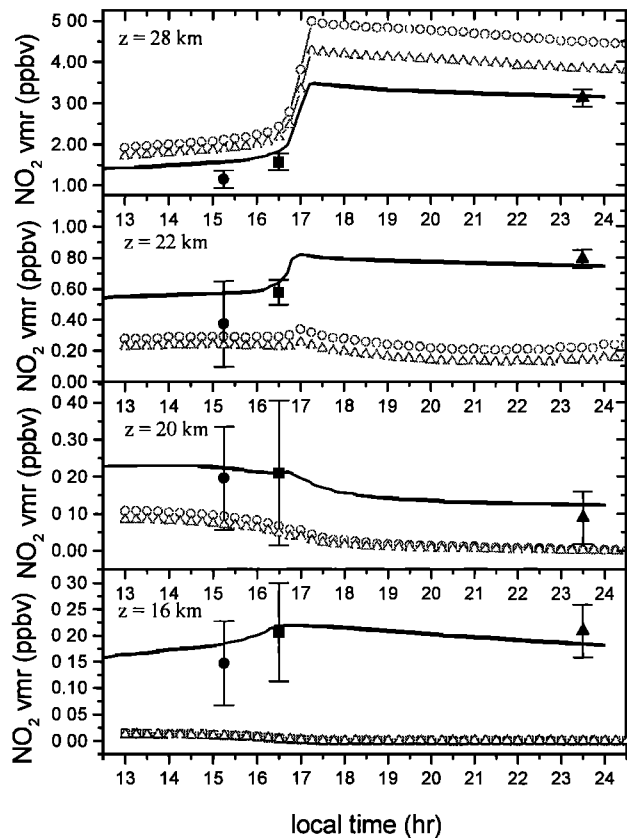
Figure 2. NO$_2$ variation with time for the altitudes 16, 20, 22 and 28 km as predicted by a box model (black lines), by Reprobus with JPL97 (blue lines), and by Reprobus with updated rate constants (red lines). LPMA ascent measurements (boxes), LPMA occultation measurements (circles), and AMON measurements (triangles) are shown for comparison.

measurements for three different times of the diurnal/nocturnal cycle and for all the altitudes sampled by LPMA and AMON is rather satisfactory.

4. Comparison With the Reprobus 3-D CTM Results

The Reprobus model is a 3-D chemistry transport model which computes the time evolution of 55 stratospheric species [*Lefèvre et al.*, 1994; 1998]. The chemical package includes a comprehensive treatment of gas-phase chemistry (147 reactions and photolysis rates from JPL97 [*De More et al.*, 1997]), as well as heterogeneous reactions taking place at the surface of liquid PSCs [*Carslaw et al*, 1995]. The model was initialized at the beginning of the winter. The wind and temperature fields used to drive the transport of chemical species and to compute the chemical rates have been prescribed every 6 hours by the ECMWF analysis and interpolated in time and space to match the Reprobus grid points. In this configuration, Reprobus extends on 31 vertical levels from the ground up to 10 hPa, with a horizontal resolution of 2° × 2°, and a chemical time step of 15 min.

Figure 1 compares the HCl Reprobus profile interpolated in space at the location of the LPMA occultation measurements (i.e., 66.9°N, 19.8°E). The model results show a significant HCl removal in the lower stratosphere, but not as large as suggested by the LPMA profile. However, it must be noted that the flight

took place close to the edge of the polar vortex, in a region where the CTM indicates a latitudinal gradient. It can be seen that at 70°N (Figure 1), about 1 grid box farther north than the LPMA flight, the heterogeneous process was more substantial in the simulations. At this latitude the modeled HCl depletion is closer to what is observed in the LPMA profile. Let us recall that the partition between HCl and ClONO$_2$ had been successfully modeled with Reprobus for a previous flight in the Arctic [*Payan et al.*, 1998]. The fact that the chemically perturbed region is located in the model further north than in the observations also explains the overestimation of ozone seen above 20 km in Plate 2.

The comparison between NO$_2$ measurements of LPMA at sunset, AMON at night, and Reprobus simulation is shown in Figure 3. Below 25 km, NO$_2$ is underestimated by Reprobus, whereas it is overestimated above as compared to LPMA and AMON measurements.

Plate 3 compares the HNO$_3$ vertical profile measured by LPMA and ILAS and the corresponding Reprobus calculation. Between 17 and 23 km, the model underestimates HNO$_3$, whereas the opposite is observed outside this altitude range.

5. Discussion

The rapid time variation of NO$_2$ prevents a direct comparison of the LPMA and AMON measurements and, as illustrated in
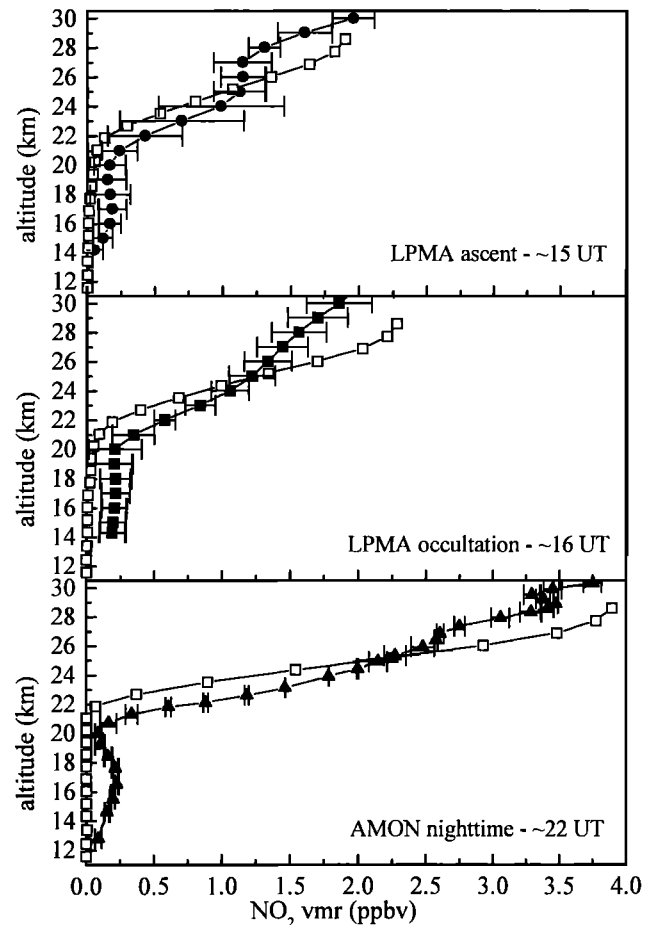

Figure 3. Comparison of NO$_2$ Reprobus (JPL97 constants, open squares) with the measurements of LPMA during ascent (SZA = 83°, black boxes), LPMA during occultation (SZA = 90°, black circles), and AMON during the night (black triangles).

Plate 1, the largest amounts of NO$_2$ were recorded by AMON during the night when photodissociation is no longer active. But, using the box model with the constraints discussed above, the nighttime AMON measurements of NO$_2$ have been converted back to the LPMA occultation measurement time. Figure 4 presents the converted AMON NO$_2$ profile and the occultation LPMA profile (corrected from photochemical effects, see section 2.1 above). It can be seen that the agreement between the two profiles is now particularly good (average difference less than 9%). Small differences can be assigned to the insufficient knowledge of J$_{NO2}$ (R1) but also to uncertainties in the chemistry and/or to the partitioning of chlorine species discussed above. As illustrated in Figure 2, knowing the NO$_2$ vmr for SZA = 90°, our 24 hour box model integration is able to simulate the observed NO$_2$ variation at any altitude during sunset and during the night, and to reproduce reasonably well the LPMA and AMON measurements. This is possible, however, with only a small degree of chlorine activation at initialization. This is not in agreement with the rather elevated Reprobus level of ClO (~350 pptv at 21 km), an overestimation also contributing (through reaction (R7)) to the low values of NO$_2$ calculated by the CTM below 25 km.

The observed partitioning between NO$_2$ and HNO$_3$ is now compared to the seasonal CTM simulation taking into account stratospheric aerosols based on Stratospheric Aerosol and Gas Experiment (SAGE) II observations [*Thomason et al.*, 1997] as well as the synoptic formation of PSCs according to the formulation of *Carslaw et al.* [1995]. The vertical distribution of the [NO$_2$]/[HNO$_3$] ratio obtained from LPMA measurements and Reprobus shows a good agreement above 22 km (Figure 5), suggesting that the NO$_y$ partitioning is properly accounted for by the model in the middle stratosphere. Therefore the overestimation of NO$_2$ by Reprobus above 25 km is probably explained by a too large NO$_y$ content at initialization and by the extrapolation of the NO$_y$ mixing ratios above the upper boundary of the model at 10 hPa (i.e., around 29 km)

Below 22 km, the [NO$_2$]/[HNO$_3$] ratio calculated by the CTM is close to zero. This results from the complete heterogeneous conversion of N$_2$O$_5$ (the usual NO$_x$ reservoir) into HNO$_3$. The well-established probability value of 0.1 for this reaction [*De*
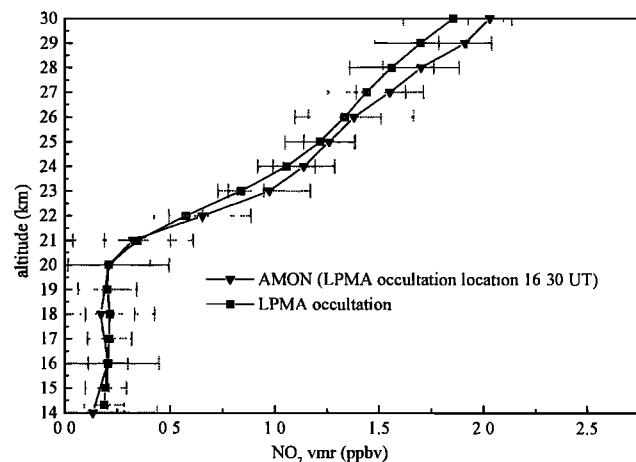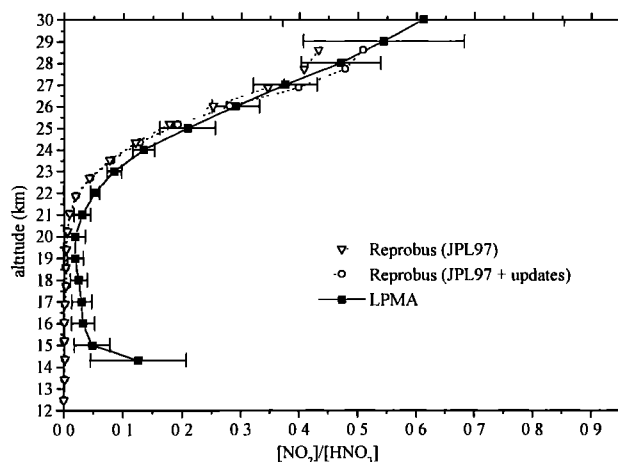
Figure 5. LPMA occultation measurements of the [NO$_2$]/[HNO$_3$] ratio between 14 and 29 km (black boxes) compared to Reprobus modeling with JPL97 (open magenta squares) and with updated rate constants (open blue circles).

More et al., 1997] and the realistic aerosol distribution used suggest that another pathway to produce NO$_2$ is lacking in the CTM.

The large amounts of HNO$_3$ measured by LPMA and ILAS are a potentially significant source of NO$_2$. The conversion in the CTM of a small amount of HNO$_3$ into NO$_2$ would not change significantly the HNO$_3$ vmr (within the error bars of the measurements; see Plate 3) while improving the agreement for NO$_2$. As an example, the conversion of 0.4 ppbv of HNO$_3$ into NO$_2$ would produce an exact agreement with LPMA at 22 km altitude and 16 30 hours (see Figure 2) while also improving the agreement with AMON NO$_2$ at 23 30 hours. Below 17 km, the conversion of HNO$_3$ into NO$_2$ would improve the modeling of both NO$_2$ and HNO$_3$.

Although the model simulation indicates that HNO$_3$ photolysis and its reaction with OH represent less than 5% of the total production of NO$_x$ below 28 km for 90° SZA, uncertainties in the gas-phase chemistry could explain part of the NO$_x$ underestimation by the model [*Sen et al.*, 1998]. Recently, the rate coefficients for O + NO$_2$ [*Gierczak et al.*, 1999] and OH + HNO$_3$ [*Brown et al.*, 1999a] reactions were reported to be significantly higher than previously recommended, while the OH + NO$_2$ reaction [*Brown et al.*, 1999b] was found to be slower than reported by *DeMore et al.* [1997]. These updates in the gas-phase chemistry, when implemented in Reprobus, do improve the results for HNO$_3$ and the [NO$_2$]/[HNO$_3$] ratio above 25 km (see Plates 3 and Figure 5), whereas they lead to very small changes below that altitude.

Alternatively, *Lary et al.* [1997] have suggested that heterogeneous processes occurring on the surface of carboneous soot particles may convert HNO$_3$ to NO$_2$. However, modeling studies [*Aumont et al.*, 1999] suggest that, like the reaction NO$_2$ + soot, the reaction HNO$_3$ + soot may be slower than expected. Another reaction not included in Reprobus is the heterogeneous conversion of formaldehyde on H$_2$SO$_4$/HNO$_3$/H$_2$O aerosol, possibly leading to an additional conversion of HNO$_3$ into NO$_2$ in the stratosphere [*Iraci and Tolbert*, 1997]. Therefore the larger aerosol load at the lower altitudes could explain higher NO$_2$ values if an additional heterogeneous reaction involving HNO$_3$ to produce NO$_2$ would be added in the model. If this process could act rapidly enough to compete with the different reactions

Figure 4. Comparison of NO$_2$ LPMA occultation measurements (corrected from photochemical variation for SZA = 90°) and AMON measurements converted to LPMA occultation time using a box model.

resulting in a loss of NO_2, it would offer an explanation for the underestimation of NO_2 by the model below 22 km.

6. Conclusion

We have presented new measurements of the NO_2 vertical distribution performed on the same day (February 26, 1997) inside the polar Arctic vortex in late afternoon, at sunset and 5 hours later during the night using the balloon-borne instruments LPMA and AMON, in the framework of the ILAS validation balloon campaign in February 1997 from Kiruna, Sweden (68°N, 21°E). In addition, LPMA measurements of O_3, HCl, and HNO_3 have been considered for comparison with models and to constrain them.

A 24 hour box model integration has been successfully used to scale the AMON nocturnal measurements to diurnal LPMA measurements. A noticeable dip is observed in the LPMA measured HCl profile, suggesting previous chlorine activation. However, in order to reproduce simultaneously the LPMA and AMON profiles, the box model has to be initialized with low ClO amounts, hence high $ClONO_2$. This could be explained by the fast deactivation of chlorine species to $ClONO_2$ buffering chlorine before final conversion to HCl.

Comparisons of these results with seasonal Reprobus simulations show an underestimation of NO_2 below 25 km, during the day and during the night. In terms of NO_y partitioning, the calculated $[NO_2]/[HNO_3]$ ratio is close to zero below 22 km. This suggests that a possible source of NO_2 is not included in the model. A change in the rate coefficients for the reaction OH + HNO_3 [*Brown et al.*, 1999a], when implemented in the chemical model, only slightly reduces the disagreement with the measurements and does not improve significantly the partitioning between NO_2 and HNO_3 below 22 km. Thus, further laboratory studies are needed to quantify more precisely other possible processes converting HNO_3 into NO_2.

Even if global measurements of NO_2 from space by the ILAS experiment are not yet fully reliable in the lower stratosphere (because they need improvement in the knowledge of the spectral dependence of the aerosol extinction coefficient), the HNO_3 measurements by ILAS provide a particularly interesting source of data to improve the modeling of HNO_3 and to test its possible contribution to the NO_2 burden. The ILAS measurements of O_3 also provide an interesting and extensive data set for the winter 1996/1997 at high northern latitudes.

New simultaneous measurements of the full suite of ClO_y and NO_y species are necessary to clarify the origin of the differences between model and observations, and a suite of dedicated balloon payloads to reach this objective is planned in the near future within several projects funded by the European Commission.

References

Aumont, B., S Madronich, M. Ammann, M. Kalberer, U. Baltensperger, D. Hauglustaine, and F. Brocheton, On the NO_2 + soot reaction in the atmosphere, *J. Geophys. Res.*, *104*, 1729-1736, 1999.

Brasseur, G, and S. Solomon, Aeronomy of the Middle Atmosphere, *Atmos. Sci. Libr.*, 441 pp, D. Reidel, Norwell, Mass., 1986.

Brown, S S, R K Talukdar and A. R Ravishankara, Reconsideration of the rate constant for the reaction of hydroxyl radicals with nitric acid, *J. Phys. Chem.*, in press, 1999a.

Brown, S S, R K Talukdar, and A.R. Ravishankara, Rate constants for the reactions OH + NO_2 + M → HNO_3+ M under atmospheric conditions, *Chem. Phys. Lett.*, *299*, 277-284, 1999b.

Camy-Peyret, C., Balloon-borne Fourier transform spectroscopy for measurements of atmospheric trace gases, *Spectrochim. Acta, 51A*, 1143-1152, 1995

Carlotti, M, Global fit approach to the analysis of limb-scanning atmospheric measurements, *Appl. Opt.*, *27*, 3250-3254, 1988.

Carslaw, K. S., B Luo, and T. Peter, An analytic expression for the composition of aqueous HNO_3-H_2SO_4 stratospheric aerosols including gas phase removal of HNO_3, *Geophys. Res. Lett.*, *22*, 1877-1880, 1995.

De More, W.B., S.P. Sander, D.M. Golden, R.F. Hampson, M.J. Kurylo, C.J Howard, A.R. Ravishankara, C.E. Kolb, and M.J. Molina, Chemical kinetics and photochemical data for use in stratospheric modeling, *JPL Publ., 97-4*, 266 pp, 1997.

Flaud, J.-M., C. Camy-Peyret, J.W. Brault, C.P Rinsland, and, D. Cariolle, Nighttime and daytime variation of atmospheric NO_2 from ground based infrared measurements, *Geophys. Res. Lett.*, *15*, 261-264, 1988.

Gierczak T., J.B. Burkholder, and A.R. Ravishankara, Temperature dependent rate coefficient for the reaction $O(^3P)$ + NO_2 → NO + O_2, *J. Phys. Chem.*, *103*, 877-883, 1999.

Glatthor, N., C.E. Blom, T. von Clarmann, H. Fischer, T. Gulde, C. Piesch, F. Erle, K. Pfeilsticker, M.P. Chipperfield, A.M. Lee, and J.A. Pyle, Airborne remote sensing of NO_2 in the Arctic winter of 1994-1995 and comparison with a three-dimensional chemical transport model, *J. Geophys. Res.*, *103*, 13315-13326, 1998.

Harder, J W., J W. Brault, P.V. Johnston, and G H. Mount, Temperature dependent NO_2 cross sections at high spectral resolution, *J. Geophys. Res*, *102*, 3861-3879, 1997.

Iraci, L.T and Tolbert M A., Heterogeneous interaction of formaldehyde with cold sulfuric acid: Implications for the upper troposphere and lower stratosphere. *J. Geophys. Res.*, *102*, 16099-16107, 1997.

Kanzawa, H., C. Camy-Peyret, Y Kondo, and N. Papineau, Implementation and first scientific results of the ILAS validation balloon campaign at Kiruna-Esrange in February-March 1997, *Proc.* 13th ESA symposium on European rocket and balloon programs and related research, *Eur. Space Agency Spec. Publ., SP 397*, 211-215, 1997

Kerr, J.B., W F.L. Ewans, and J.C. McConnell, The effects of NO_2 changes at twilight on tangent ray NO_2 measurements, *Geophys. Res. Lett.*, *14*, 577-579, 1987.

Kondo, Y., T. Sugita, R.J. Salawitch, M Koike, and T. Deshler, The effect of Pinatubo aerosols on stratospheric NO, *J. Geophys. Res.*, *102*, 1205-1213, 1997

Lary, D.J., R. Toumi, A M Lee, M. Newchurch, M. Pirre, and J.B Renard, Carbon aerosols and atmospheric photo-chemistry, *J. Geophys. Res.*, *102*, 3671-3682, 1997

Lefèvre, F., G. Brasseur, I. Folkins, A.K Smith, and P. Simon, Chemistry of the 1991-1992 stratospheric winter Three dimensional model simulations, *J. Geophys. Res.*, *99*, 8183-8195, 1994.

Lefèvre, F., F. Figarol, K.S Carslaw, and T. Peter, The 1997 Arctic ozone depletion quantified from three-dimensional model simulations, *Geophys. Res. Lett.*, *25*, 2425-2428, 1998

Naudet, J P., C. Robert, and D Huguenin, Balloon measurements of stratospheric trace species using a multichannel UV-Visible spectrometer, *Proc* 11th ESA symposium on European rocket and balloon programs and related research, *Eur. Space Agency Spec. Publ., SP-355*, 165-168, 1994

Newchurch, M.J., et al, Stratospheric NO and NO_2 abundances from ATMOS solar-occultation measurements, *Geophys. Res. Lett.*, *23*, 2373-2376, 1996.

Payan S., C Camy-Peyret, P Jeseck, T. Hawat, G Durry and F. Lefèvre, First simultaneous HCl and $ClONO_2$ profile measurements in the Arctic vortex, *Geophys. Res. Letters*, *25*, 2663-2666, 1998

Press, W.H., S.A. Teukolsky, W.T. Vetterling, and B.P. Flannery, *Numerical recipes in Fortran*, 2nd ed., 963 pp., Cambridge Univ. Press, New York, 1992.

Ramaroson, R.A., M Pirre, and D. Cariolle, A box model for one-line computations of diurnal variation in a 1-D model Potential for application in multidimensionnal cases, *Ann. Geophys.*, *10*, 416-428, 1992

Renard, J.B, M Pirre, C Robert, D. Huguenin, G. Moreau, and J M. Russel, Nocturnal distribution of stratospheric O$_3$, NO$_2$ and NO$_3$ from balloon measurements, *J. Geophys. Res., 101*, 28793-28804, 1996.

Robert, C., Réalisation d'un spectromètre stellaire multicanal embarquable sous ballon stratosphérique, Ph.D thesis, Univ. of Orléans, Orléans, 1992.

Russel, J.M., III, C.B. Farmer, C.P. Rinsland, R. Zander, L. Froidevaux, G.C. Toon, B Gao, J Shaw, and M. Gunson, Measurements of odd nitrogen compounds in the stratosphere by ATMOS experiment on spacelab 3, *J. Geophys. Res., 93*, 1718-1736, 1988.

Sasano, Y, M. Suzuki, T. Yokota, and H. Kanzawa, Improved Limb Atmospheric Spectrometer (ILAS) for stratospheric ozone layer measurements by solar occultation technique, *Geophys. Res. Lett., 26*, 197-200, 1999.

Sen, B, G.C Toon, G.B. Osterman, J.-F. Blavier, J.J. Margitan, R.J Salawitch, and G.K. Yue, Measurements of reactive nitrogen in the stratosphere, *J. Geophys. Res., 103*, 3571-3585, 1998.

Thomason, L.W., L.R. Poole, and T.R. Deshler, A global climatology of stratospheric aerosol surface area density as deduced from SAGE II: 1984-1994, *J. Geophys. Res., 102*, 8967-8976, 1997.

Webster, C.R., R.D. May, M. Allen, L. Jaeglé, and M.P. McCormick, Balloon profiles of stratospheric NO$_2$ and HNO$_3$ for testing the heterogeneous hydrolysis of N$_2$O$_5$ on sulfate aerosols, *Geophys. Res. Lett., 21*, 53-56, 1994.

Wetzel, G., H. Oelhaf, T. von Clarmann, H. Fischer, F. Friedl-Vallon, G.

Maucher, M Seefeldner, and O Trieschmann, Vertical profiles of N$_2$O$_5$, HO$_2$NO$_2$, and NO$_2$ inside the Arctic vortex retrieved from nocturnal MIPAS-B2 infrared limb emission measurements in February 1995, *J. Geophys. Res., 102*, 19177-19186, 1997

Yokota, T., M. Suzuki, O.V Duvobik, and Y. Sasano, ILAS (Improved Limb Atmospheric Spectrometer)/ADEOS data retrieval algorithms, *Adv. Space Res., 21*(3), 393-396, 1998.

C. Camy-Peyret, P. Jeseck, and S. Payan, LPMA, UPMC/CNRS, 4 place Jussieu, Bte 76, 75252 Paris cedex 05, France. (payan@ccr.jussieu.fr)

T. Hawat, University of Balamand, Faculty of Engineering, P.O. Box 100 Tripoli, North Lebanon, Beirut, Lebanon. (hawat@ccr jussieu.fr)

H. Kanzawa, and Y. Sasano, National Institute for Environmental Studies, 16-2 Onogawa, Tsukuba, Japan (kanzawa@nies.go.jp)

F. Lefèvre, CNRS Service d'Aéronomie, Université Pierre et Marie Curie, BP 102, 4 Place Jussieu, 75252 Paris Cedex 05, France (franck.lefevre@aero.jussieu.fr)

M. Pirre, J.-B. Renard, and C Robert, LPCE-CNRS, 3A Avenue de la recherche scientifique, 45071 Orléans cedex 2, France. (mpirre@cnrs-orleans.fr)